

LETTER

Linking canopy leaf area and light environments with tree size distributions to explain Amazon forest demography

Scott C. Stark,^{1,2*} Brian J. Enquist,^{1,3} Scott R. Saleska,¹ Veronika Leitold,⁴ Juliana Schiatti,⁵ Marcos Longo,⁶ Luciana F. Alves,^{7,8} Plinio B. Camargo⁹ and Raimundo C. Oliveira¹⁰

Abstract

Forest biophysical structure – the arrangement and frequency of leaves and stems – emerges from growth, mortality and space filling dynamics, and may also influence those dynamics by structuring light environments. To investigate this interaction, we developed models that could use LiDAR remote sensing to link leaf area profiles with tree size distributions, comparing models which did not (metabolic scaling theory) and did allow light to influence this link. We found that a light environment-to-structure link was necessary to accurately simulate tree size distributions and canopy structure in two contrasting Amazon forests. Partitioning leaf area profiles into size-class components, we found that demographic rates were related to variation in light absorption, with mortality increasing relative to growth in higher light, consistent with a light environment feedback to size distributions. Combining LiDAR with models linking forest structure and demography offers a high-throughput approach to advance theory and investigate climate-relevant tropical forest change.

Keywords

Amazon forest, canopy plasticity, canopy structure, forest dynamics, leaf area profiles, LiDAR, light competition, metabolic scaling theory, remote sensing, tree demography.

Ecology Letters (2015) 18: 636–645

INTRODUCTION

Current ecological theory holds that light is a limiting resource in forests, influencing tree dynamics through gap forming mortality events (Brokaw 1985; Clark & Clark 1992; Chambers *et al.* 2004; Grote *et al.* 2013). Generally, a feedback between forest structure – which influences light environments – and tree growth and survival may control forest dynamics (Kohyama 1993; Moorcroft *et al.* 2001). To investigate this feedback in forests where light environments are difficult to measure directly, light has been assumed to increase with height and decrease with neighborhood basal area (Kohyama 1993; Moorcroft *et al.* 2001; Muller-Landau *et al.* 2006a, b; Purves *et al.* 2007; Strigul *et al.* 2008). The alternative approach of metabolic scaling theory (MST) assumes that competition for space explains forest dynamics (Enquist *et al.* 2009; West *et al.* 2009). Improving understanding of the feedback between forest structure and dynamics is crucial for prediction of responses to disturbances such as drought-related

large tree mortality in the Amazon (Phillips *et al.* 2009) and to improve next generation models of vegetation–atmosphere interactions (Moorcroft *et al.* 2001; Moorcroft 2006; Sitch *et al.* 2008; Medvigy *et al.* 2009).

Here, we take an approach that uses LiDAR remote sensing and coincident forest plot surveys to retrieve both fine scale data on canopy structure (Harding *et al.* 2001; Parker *et al.* 2001, 2004; Drake *et al.* 2002; Lefsky *et al.* 2002; Kellner & Asner 2009, 2014; Stark *et al.* 2012) and information on light environments (Parker *et al.* 2001; Stark *et al.* 2012). We developed a new model that linked leaf area profiles and tree size distributions with canopy light environments. We then assessed the role of light limitation in tree growth and mortality by estimating the specific light environments experienced by different tree size classes from the model.

This study developed a detailed quantitative connection between canopy leaf area and light environments (canopy structure), the numbers and sizes of trees (size structure), and tree vital rates (demographic dynamics) that spanned the tree

¹Department of Ecology and Evolutionary Biology, University of Arizona, Tucson, AZ, 85721, USA

²Department of Forestry, Michigan State University, East Lansing, MI, 48824, USA

³The Santa Fe Institute, 1399 Hyde Park Road, Santa Fe, NM, 87501, USA

⁴Instituto Nacional de Pesquisas Espaciais (INPE), São José dos Campos, São Paulo, 12201-970, Brazil

⁵Coordenação de Pesquisa em Biodiversidade, Instituto Nacional de Pesquisas da Amazônia (INPA), Manaus, Amazonas, 69011-970, Brazil

⁶Faculty of Arts and Sciences, Harvard University, Cambridge, MA, 02138, USA

⁷Centro de Pesquisa e Desenvolvimento de Recursos Genéticos Vegetais, Instituto Agronômico de Campinas (IAC), CP 28, Campinas, São Paulo, 13012-970, Brazil

⁸Departamento de Biologia Vegetal, Universidade Estadual de Campinas (UNICAMP), CP 6109, Campinas, São Paulo, 13093-970, Brazil

⁹Laboratório de Ecologia Isotópica, Centro de Energia Nuclear na Agricultura (CENA), Universidade de São Paulo, Piracicaba, São Paulo, 13400-970, Brazil

¹⁰NAPT Médio Amazonas, Embrapa Amazônia Oriental, Santarém, Pará, 68035-110, Brazil

Biospheric Sciences Laboratory, NASA Goddard Space Flight Center, Greenbelt, MD, 20771,

Monitoramento por Satélite, Empresa Brasileira de Pesquisa Agropecuária (Embrapa), Campinas, São Paulo, 13070-115, Brazil

*Correspondence: E-mail: scott.c.stark@gmail.com

size spectrum. It also demonstrated the retrieval of tree size distributions and size-structured tree demographic dynamics from LiDAR data.

METHODS

Approach

MST offers a foundation for connecting tree size structure with the space occupancy of tree crowns in the canopy, predicting from optimality principles that crowns scale with diameter according to specific power function (log–log linear) allometries (Enquist *et al.* 1999; Enquist *et al.* 2009; West *et al.* 2009; Coomes *et al.* 2012). MST has been extended by including competition for space between like-sized tree crowns (H1: space limitation) to predict that size distributions follow a log–log linear Pareto form, which specifically displays an exponent of -2 when total tree crown leaf area limits spacing (West *et al.* 2009). An alternative demographic theory for size distributions holds that light limitation in the subcanopy may reduce the frequency of small trees, resulting in a log–log concave-down curvilinear Weibull-type size distributions (H2: light limitation Kohyama 1993; Muller-Landau *et al.* 2006b; Coomes *et al.* 2011).

Step A: We compared models that related canopy and size structure. Models were comprised of architectural rules – including allometries – that governed the vertical locations of leaves of specific tree size classes in the canopy. The objective was to predict size structure from LiDAR observations of vertical canopy structure. We compared a model (Model I) that was based on restrictive MST crown scaling assumptions with another (Model II) that relaxed these assumptions to allow light to influence canopy architecture. Canopy architecture may vary as a function of adult stature, light demand and light environment in tropical trees (Sterck & Bongers 2001; Poorter *et al.* 2003), while crowns may preferentially occupy high light environments (Young & Hubbell 1991). We tested the hypothesis that canopy architecture was plastic (H3) by comparing versions of Model II that included different rules allowing light to influence the relationship between canopy and size structure, including a version with no dependency of canopy architecture on light.

Step B: We next quantitatively predicted the light environments of the leaf area associated with different tree size classes, using our best forest structure model from Step A and taking into account the complex vertical overlap of size classes in leaf area profiles. We then tested two predictions from the hypotheses above: Under MST the ratio of mortality rate to relative growth rate (henceforth ‘demographic ratio’) is constant over light environments and tree diameter (prediction H1; Muller-Landau *et al.* 2006b). In contrast, light limitation of growth or mortality rates may cause the demographic ratio to increase or decrease over light, depending on the specific impacts of light, influencing size distributions (prediction H2; Muller-Landau *et al.* 2006b). We asked if potential light dependence of growth, mortality and the demographic ratio was consistent with size distributions at sites, employing equilibrium forest demographic theory (Kohyama 1993).

Study sites, tree inventory plots, and demographic rates

We considered 38 one-hectare (1 ha) long-term forest inventory plots from two sites in the central Amazon – 22 plots from Adolfo Ducke Reserve (Manaus, Amazonas, Brazil) and 16 from the Tapajós National Forest (Santarém, Pará, Brazil, ~ 600 km east of Manaus; Rice *et al.* 2004; Vieira *et al.* 2004; Magnusson *et al.* 2005; Castilho *et al.* 2006; Pyle *et al.* 2008). Both sites are *terra firme* forest while the Tapajós has a stronger dry season (5 month vs. 3 month < 100 mm rainfall month $^{-1}$). While shorter by ~ 10 m, the canopy of Ducke more rapidly reduces light to low levels relative to the Tapajós due to the presence of a developed upper canopy layer; the Tapajós is characterised by an open heterogeneous upper canopy, relatively constant light absorption, and gradually decreasing leaf area density with height (Stark *et al.* 2012). Prior studies and preliminary analysis revealed heterogeneity in canopy and size structure between plots and sites (Pyle *et al.* 2008; Stark *et al.* 2012 see also Figs S3, S5 and S6).

Plots were rectangular, 250 m long, and overlapping for small, medium and large trees. Ducke size classes were 1–10 cm DBH, 10–30 cm DBH, and > 30 cm with areas of 4×250 , 20×250 , and 40×250 m respectively, while Tapajós size classes were 10–35 cm and trees > 35 cm DBH with areas of 10×250 and 50×250 m respectively (Rice *et al.* 2004; Castilho *et al.* 2006). Ducke plots followed topographic contours and were separated by 1 km (Magnusson *et al.* 2005; Castilho *et al.* 2006) while Tapajós plots were adjacent on the shortest plot dimension in the footprint of an eddy-covariance tower (Rice *et al.* 2004; Pyle *et al.* 2008). After measurement of DBH, tree frequencies in the different plot sizes were standardised to one hectare. We defined a ‘size group’ of trees as individuals that fell within a particular DBH size bin *within a particular plot*, spanning 10–200 cm DBH in steps of 3 1/3 cm – this small diameter bin width improved the stability of model fitting.

We quantified demographic rates from tree inventory data at both sites. Tapajós plots were surveyed every other year from 1999 to 2005 and annually from 2006 to 2011. Ducke plots were surveyed in 2001, 2003, and 2007. Normalised diameter growth was calculated for all intervals and individuals. Potential growth outliers were removed. We fit growth and mortality vs. diameter relationships to individual tree-level data – a locally weighted polynomial curve predicted tree growth while mortality was modelled by a power function of diameter with an additional quadratic term, which provided a better fit than a power law, the MST-expected relationship (West *et al.* 2009). Mortality functions were fit with maximum likelihood. Demographic ratio (mortality to relative growth) was estimated, at the site level, from the final fit growth and mortality relationships.

LiDAR-based leaf area and light estimation

Sites were overflown with a discrete-return small-footprint Leica Geosystems ALS70-II LiDAR (Heerbrugg, Switzerland) in June 2008 with pulse densities averaging 50 per m 2 . Due to plot geometry, we extracted the central 10 m wide swath of

LiDAR data within the plot, which likely maximises the correspondence of canopy structure and tree surveys. Plot and LiDAR data geospatial correspondence was established from GPS measurements and a distance-decay correlation analysis of ground-based and airborne-LiDAR data on canopy height (Supplementary Information, SI, 1.1; Stark *et al.* 2012).

To derive mean leaf area density profiles from LiDAR in these plots Stark *et al.* (2012) employed the MacArthur–Horn method (MacArthur & Horn 1969). The average proportional transmittance of incident light ('light profile', I) and the average absorption of light in canopy voxels ('absorption profile', ΔI) were estimated by applying a vertical light reduction model to leaf area density estimates (Stark *et al.* 2012). For detailed information, validation analysis, and related approaches see SI 1.2, Stark *et al.* (2012) and other studies (Harding *et al.* 2001; Parker, *et al.*, 2001, 2004; Drake *et al.* 2002; Tang *et al.* 2012).

Canopy structure to size distributions (Step A)

We considered two models, based on differing assumptions, that mechanistically linked canopy leaf area profiles with size distributions ('forest structure models'). The first model was based on MST and encompassed a restrictive set of allometric scaling assumptions (SI 1.4, 'Model I'; Enquist, *et al.* 1999, 2009; West *et al.* 2009). This model allowed us to uniquely explore the quantitative expectation for canopy structure (the leaf area profile) under MST ideal size distributions (SI 1.4; Fig. S2). The second model relaxed the MST assumption that crown architecture depends on tree size alone by incorporating plastic crown geometrical responses to light (SI 1.5, 'Model II'). In this case, leaf or whole-crown position responded to light (H3), which was estimated from LiDAR (Stark *et al.* 2012).

Forest structure model I

Model I assumed that (1) tree crowns were cylindrical solids with dimensions that changed proportionally with canopy volume, that (2) height and diameter were related to a power function allometry characterised by normalisation and scaling parameters (see Feldpausch *et al.* 2010), that (3) leaf area density (LAD, m^2 leaf area per m^3 canopy volume) was constant within crowns and (4) that total leaf area \propto basal area (Shinozaki *et al.* 1964; Enquist & Niklas 2002). We applied the model over tree survey data to predict leaf area density profiles, which we compared with LiDAR observations. Since model assumptions govern individual tree crowns the model has the potential to predict site differences in canopy structure even if size distributions differ from the optimal MST expectation. We also calculated an exact numerical prediction for the leaf area profile under ideal MST size distribution: $\text{LAD} \propto H^{1/2}$, where H is height in the canopy (SI 1.4).

The model was fit with nonlinear least squares minimisation. We compared only the regions of leaf area density profiles above 12 m to minimize the potential effect of a 10 cm DBH minimum tree size cutoff (for all analyses) – trees < 10 cm are unlikely to contribute significantly to vegetation at this height (Feldpausch *et al.* 2010).

Forest structure model II, including plasticity of crown architecture

Model II predicted tree size distributions from LiDAR observations of canopy structure, specifically leaf area and light profiles. The key feature of this model was that it predicted the contribution of each tree size group to forest structure. The model simultaneously predicted leaf area density profiles and frequencies of individuals in size groups from a series of structural rules relating these variables, which were processed when the model was applied to LiDAR data. Four optional structural rules related aspects of each size group's leaf area profile with light environment estimates. During model development, these rules were included, or left out, based on a comprehensive model fitting and comparison analysis. The total leaf area, the vertical distribution of leaf area, and the frequency of individuals in each size group were constrained by LiDAR data and the structural rules retained after model selection. Figure 1, Table 1 and SI 1.5 provide additional description of Model II.

The work-flow for the application of the model to LiDAR data was to: (1) process rules to determine the *relative* vertical distribution of leaf area for each size group, including applying rules assigning the vertical distribution of leaf area from light profiles estimated with LiDAR; (2) solve for the total leaf area in each size group by inverting a linear matrix model to relate observed plot-level leaf area profiles to predicted leaf area profiles from size groups; (3) predict stem densities in each size group from the total basal area, which was assigned by a rule that allometrically relates leaf area with basal area; (4) based on the predicted stem density distribution and the associated predicted leaf area density profile, calculate the likelihood of the data given the model. A final step multiplied the size distribution by an adjusted constant that scaled the distribution to total tree density in one hectare plots.

Vertical distributions of leaf area were calculated for size groups from the following assumptions and rules: We assumed that there is an underlying vertical distribution of leaf area origin points in the canopy – conceptually, these origin points correspond with tree crown bases or branching points. The vertical frequencies of origin points were modelled as a truncated gamma probability distributions, which can take a wide range of configurations with two parameters. Maximum heights of origin points were constrained to fall at or below maximum tree heights, which were calculated from a height-diameter allometry that was fit as a model component. Leaf area was arrayed upward from origin points according to a linear dependency on light environment estimates when optional Rule III was active (Table 1, SI 1.5) – this allowed for varied and multimodal leaf area profiles to emerge from the influence of light profiles. Three additional optional rules related leaf area with light but relied on reference light estimates taken at the tops of crowns for each size group (Table 1, SI 1.5). Corresponding Reference heights were calculated from an empirically based height-diameter allometry for the Eastern Amazon (Feldpausch *et al.* 2010). Rule I stated that the normalisation of the height-diameter allometry depended linearly on reference light, while Rule II encoded linear light

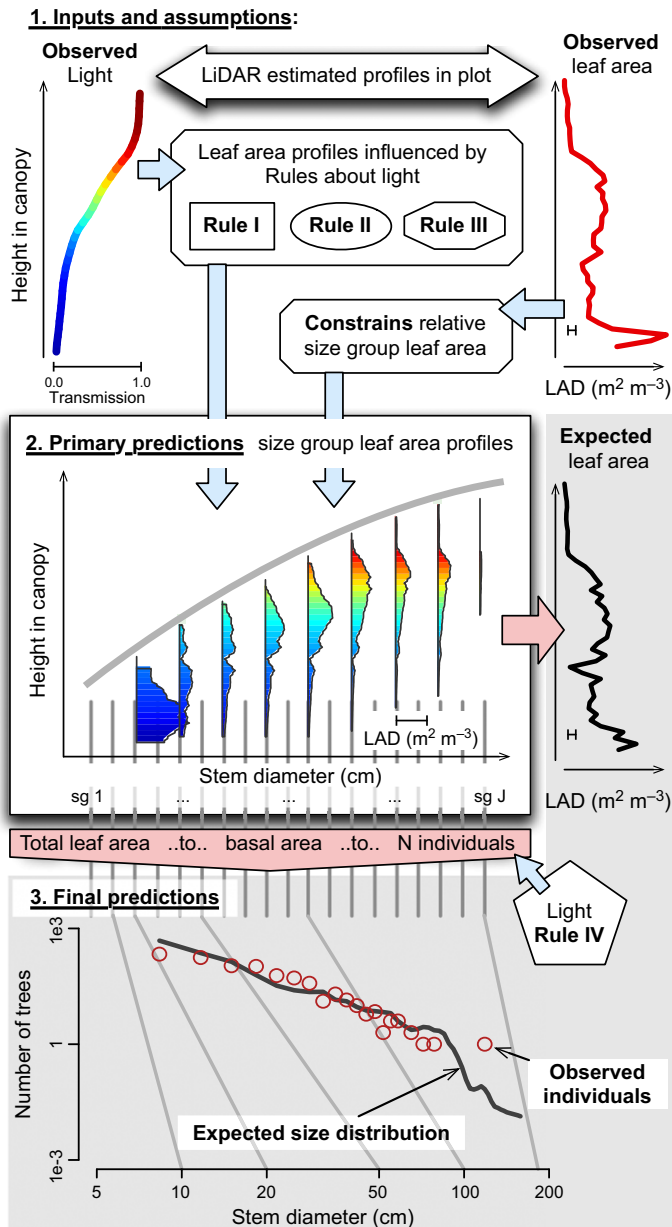


Figure 1 Forest structure Model II applied to a one-hectare forest plot. Leaf area was partitioned into overlapping size group sub-profiles according to allometric assumptions and, depending on the model version, Rules I – III including information on light environments. Observed (LiDAR-estimated) leaf area profiles constrained the relative distribution of leaf area among size groups through a model inversion calculation. The expected profile – a model ‘final prediction’ – is the sum of the sub-profiles of model ‘primary predictions’. Colors correspond with leaf light environments (LiDAR-estimated light profile provides color key). Next, the model related the total leaf area to the total basal area of size groups, which were assumed to be proportional; the proportionality constant, however, could be influenced by light (Rule IV). Dividing total size group basal area by the diameter midpoint yielded the expected number of individuals (N). Thus, the second ‘final prediction’ was the size distribution. Red circles are observed tree counts in size groups.

dependencies for both parameters of the gamma distribution. Rule IV stated that the total leaf area per unit of basal area depended nonlinearly on reference light. The model did not

explicitly consider horizontal crown plasticity (see Purves *et al.* 2007; Strigul *et al.* 2008).

We fit the model to data on one-hectare plot stem diameter distributions and leaf area density profiles with maximum likelihood analysis. We used a subset of 16 plots taken from both sites (8 from each) to fit and compare models. We compared model versions, 288 total, that incorporated different combinations of the optional rules, including a version with no light dependency, with AIC analysis, selecting the best model based on the lowest combined Δ AIC rank for size distribution and leaf area profile predictions (Table 1; SI 1.5 & 1.6). We also scaled size distributions to tree density by adjusting a constant to minimize the least squared error of predictions for the 16 model-development plots (SI 1.5). We extended the best model across all plots, including the 22 initial hold-outs, to predict size distributions and canopy profiles.

Relating light with demographic dynamics in complex canopies (Step B)

Estimating size group absorption

We next estimated light absorption per unit leaf area of each size group – a metric of the light environment – from the best forest structure model (SI 1.8). We then compared these values with tree growth and mortality rates at each site to test predictions H1 & H2 (Fig. S7; SI 1.8). We assumed that leaf area was randomly distributed over horizontal light variation across size groups. Since the largest, lowest probability, size groups may not be represented in many 1ha-plots we discounted these size groups (SI 1.8). This may have reduced accuracy of absorption estimates in remaining size groups. We used stem diameter to match the expected values from growth and mortality relationships, available only at the site-level, with all size group absorption estimates. Thus we included plot-level variation in absorption but not demography in analysis.

Demography and canopy light environments

We tested the hypothesis that variation in demographic processes over tree size classes within sites – including the relative roles of mortality and relative growth, the demographic ratio – was related to light environments. By employing forest demographic theory developed by Kohyama (1993) and elaborated by Muller-Landau *et al.* (2006b) we also asked if apparent impacts of light environments on demographic rates are consistent with site differences in size distributions. Under MST predictions the ratio of mortality to relative growth rate is expected to be a constant (Muller-Landau *et al.* 2006b). If light influences the size distribution, however, we hypothesised that the demographic ratio would be related to average leaf-level light absorption. Based on preliminary analysis we assumed a linear relationship:

$$m(D) \cdot D/g(D) = m(D)/RGR(D) \propto A(D) \quad (1)$$

where D is diameter, m and g are mortality and growth rates respectively, RGR is the relative growth rate and A is light absorption (SI 1.9). This corresponds with mortality increasing relative to growth in higher light and, on average, at larger tree sizes in the demographic model. We also assumed

Table 1 Model II rules relating LiDAR-based light estimates with size group leaf area profiles. Model II algorithmically predicted tree size distributions from LiDAR observations of leaf area and light profiles. Versions of Model II that incorporated between 0 and 4 rules and one or more of predictor variables vertical light transmission, light absorption, and size group diameter were compared with Δ AIC analysis (288 total versions). The Best Model Variable(s) column indicates which rules and variables were included in the best model, unless the rule was not supported (not included in the best model). See Methods and SI 1.5 & 1.6 for additional specification

Rule	Description	Specification*	Best model variable(s)
I	Maximum tree height is related to light environment	$H = \kappa' \cdot D^\phi$, where H and D are height and diameter and κ' was a linear function of light metrics at maximum heights	<i>Not supported</i>
II	Gamma distribution profile of crown base positions related to light	For each size group $gamma(\kappa, \theta)$, where κ and θ parameters are linear functions of predictor variables	Light transmittance at size class maximum height
III	Leaf deployment is directly related to fine scale (vertical) light transmission and absorption variation	For each size group i the leaf area profile over z height is $LAD_{z,i} = \mu_0 + \mu_1 I_z + \mu_2 \Delta I_z$, where I is light transmittance and ΔI is light absorption [†]	Light transmittance & absorption
IV	Quantity of leaf area per basal area increases over light environments	$BA = \eta' \cdot (1 + \rho V^z) \cdot LAI$, where BA and LAI are total basal area and LAI of size classes and V is a light metric	Light transmittance at size class maximum height

*All unnamed variables are fit parameters excepting η' , which was adjusted in a separate step (SI 1.5).

[†]This linear equation was applied in a stepwise manner moving up in the canopy from the base position until the size group total leaf area was reached.

equilibrium size structure at sites and that in the absence of light limitation the size distribution would follow the optimal MST prediction.

This extension of forest demographic theory provides a hypothesis for how patterns of light absorption over tree size may influence size distributions. With the assumption of eqn 1, the size distribution probability density function, $p(D)$, may be approximated by

$$p(D) = \frac{1}{K'} D^{-(A+B \cdot D)} \quad (2)$$

where A and B are constants related to a light environment vs. diameter function and K' is a scaling constant (SI 1.9). Fitting this function to site size distributions allowed us to predict relative differences in light absorption over size groups by propagating the values of A and B through the light environment vs. diameter function (SI 1.9), providing a weak test of the feedback hypothesis. If light environments are constant over size classes the exponent function, $A + B \cdot D$, is replaced by a constant and the distribution is a log–log linear Pareto form. Alternatively, if light increases over size classes then the exponent function increases with diameter and the distribution is log–log curvilinear ‘Weibull-like’.

RESULTS

Canopy structure to size distributions

Model I significantly predicted canopy profiles ($R^2 = 0.93$, $RSE = 0.026$, $P < 0.0001$, d.f. = 86). However, inspection suggested that this model failed to predict the marked differences in canopy structure between sites (Fig. S3): the model predicted that the Tapajós was taller but it failed to predict the developed upper canopy layer found in Ducke. Furthermore, vertical leaf area profiles appeared to differ from the expectation of MST under ideal crown architectural scaling and size distributions (compare Figs S2 & S3). This was consistent with the observation that size distributions differed from the

MST prediction: The Tapajós size distribution approximated a Pareto form, while displaying a scaling exponent below the expected -2 value (-2.6 ; Fig. S1; SI 1.3). Ducke approximated a Weibull distribution (Fig. S1).

The best version of Model II, selected with model comparison, provided a significantly better fit to site leaf area density profiles than Model I ($R^2 = 0.97$, $RSE = 0.018$, $P < 0.0001$, d.f. = 86; Δ AIC = 51.40; Fig. S3). This model also significantly predicted plot and site differences in size distributions and leaf area profiles with 11 parameters fit generally (Figs 2 & 3; Tables 1 & S1): Site-level size distribution predictions were significantly better than the over-all aggregate prediction (Δ AIC = 17.7) while plot-level predictions were significantly better than site-level aggregate predictions, but in this case only when we excluded trees above the 98.5th diameter quantiles of each site (Δ AIC = 137.9; SI 1.5 end & 1.6; for raw plot predictions Figs S5 & S6). The height-diameter scaling constant was similar to an empirical estimate for the Eastern Amazon (0.553 our study vs. 0.507 Feldpausch *et al.* 2010; SI 1.6).

After scaling size distributions to tree densities, we found that the best Model II version predicted 90% of the variance over all size group observations from LiDAR ($RSE = 10.25$, $P < 0.0001$, d.f. = 2164). This analysis did not account for potential spatial non-independence. The intercept and slope of the observed vs. expected regression differed from zero and one (CIs: 0.22–1.06 & 0.86–0.88), potentially indicating a $< 20\%$ over-prediction in small size groups, which were more variable.

Model II supported the plasticity hypothesis (H3): the best version of Model II included three rules linking estimated light environments with leaf area profiles (Table 1; SI 1.5). In contrast, the Model II version that included no light rules was not supported, ranking in the lowest 20% for the leaf area profile prediction (AIC comparison; SI 1.6). Together, these rules modified the vertical distribution of the origin points of leaf area in the canopy (Rule II) and related fine scale vertical variation in leaf area density to estimated light absorption

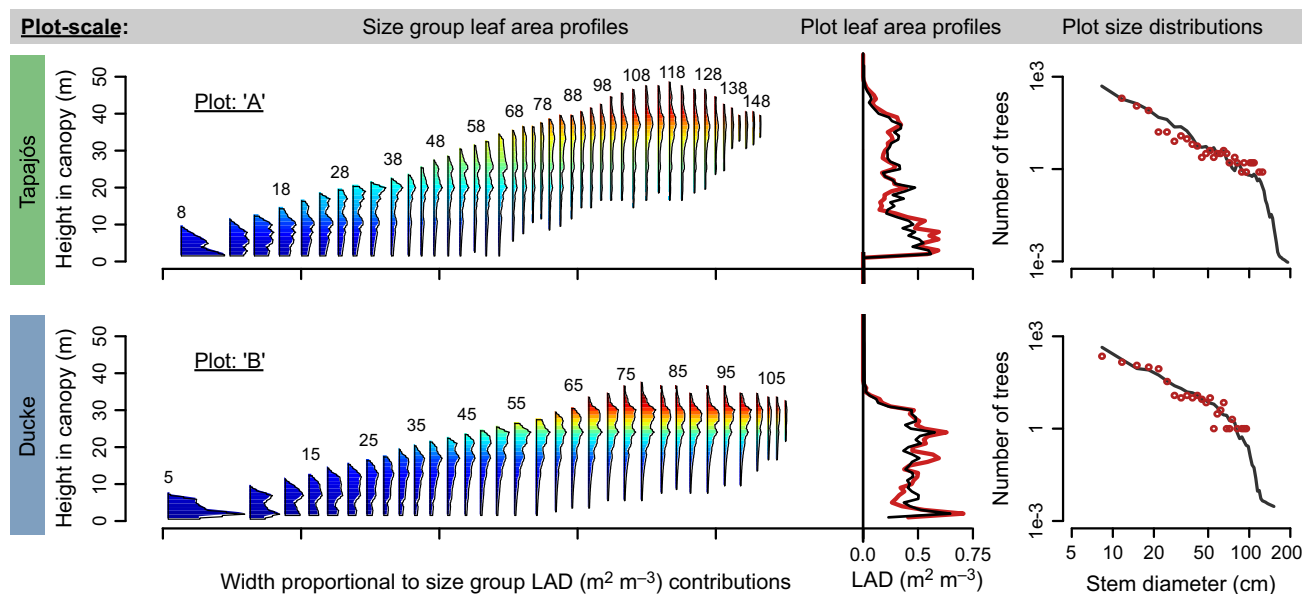


Figure 2 Plot-scale forest structure Model II predictions vs. observations, showing a single one-hectare forest plot from each site (2 of 38 plots; Figs S5 & S6). These plots, selected randomly, were not used to fit the model. The best version of Model II was applied to LiDAR-estimated profiles of leaf area density, light transmission, and light absorption to generate predictions. Panel columns are (1) size group leaf area profiles (leaf area density, LAD, m^2/m^3), (2) plot-level leaf area profiles (same units, smaller scale), and (3) size distributions (trees ha^{-1} over diameter in cm). Small numbers indicate the diameters (cm) of size group leaf area profiles. Heat colors indicate high (red) to low (blue) light transmission environments. LiDAR-estimated site leaf area profiles (red) are compared with model predictions (black). Observed tree counts in size bins (red circles) are plotted against model expectations (black lines).

and transmission (Rule III). The model also supported the influence of light on leaf allocation (Rule IV): total leaf area increased relative to basal area in higher light, with the ratio varying two-fold or less over the lower 99% of the size distribution (Fig. S7c). The net effect of these rules was to increase peakedness (kurtosis) and the height of upper leaf area quantiles in higher light environments (Fig. S4; SI 1.7), in agreement with phototrophic canopy plasticity (Monteith 1965; Horn 1971; Young & Hubbell 1991; Strigul *et al.* 2008; Coomes *et al.* 2012). Thus, leaf area was more concentrated into the upper portions of profiles that fell in higher light environments, independent of size class diameter.

Relating light with demographic dynamics in complex canopies

Growth appeared to increase and then level off over increasing light absorption classes generated from Model II predictions (Fig. 4). This pattern appeared to agree with the predictions of light limitation (H2), but over low-light variation. In addition, we observed an increasing relationship between the demographic ratio and absorption that appeared proportionally similar at both sites over much of the tree size range and was consistent with mortality increasing relative to relative growth rate over light environments (Fig. 5).

The demographic flux model (eqn 2, SI 1.9) when fit at both sites appeared to capture size distribution log–log curvature (Fig. S1, right column). Consistent with the expectations of this model, the more Pareto-like Tapajós size distribution was associated with a more constant, or ‘slowly increasing’, light absorption pattern with tree size, while the Weibull-like

Ducke size distribution was associated with a steeper increase in absorption with tree size (SI 1.9; Fig. S8).

DISCUSSION

We found that the structure of Amazon forest canopies – the distributions of leaf area and light environments – was integrally connected to size (diameter) distributions of trees. Because of this connection it was possible to predict tree size distributions from LiDAR remote sensing of vertical components of canopy structure. Light was a critical component of this connection. Models that included information on leaf light environments significantly improved predictions of leaf area profiles and size distributions relative to models that did not. Combined with analysis of model output of the leaf area profiles of size groups in different light environments – showing more upwardly peaked profiles in higher light – this comparison provided support for phototrophic canopy plasticity (H3; Monteith 1965; Horn 1971; Young & Hubbell 1991).

Model rules that incorporated information on light environments allowed leaf area to track canopy environments and accurately predict an upper canopy layer in the Ducke site and the absence of one in the Tapajós. The model based on invariant MST crown scaling relationships, in contrast, erroneously predicted that both Ducke and Tapajós leaf area profiles resembled the Tapajós pattern of gradually decreasing leaf area density with height. Phototrophic canopy plasticity is the most likely explanation for the deviation of Ducke from the invariant scaling model. Thus, as a dense canopy developed through time in this forest, rapid light reduction may

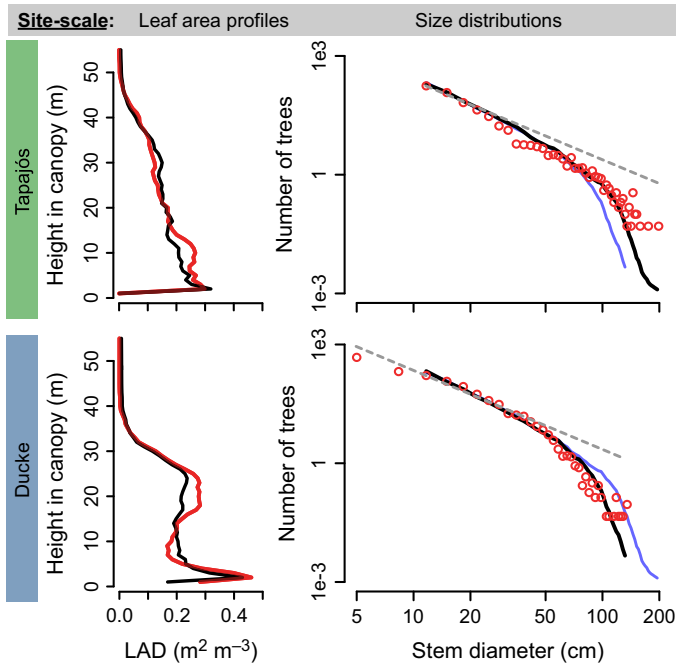


Figure 3 Site-scale Model II forest structure predictions and observations for leaf area profiles (left column of figures) and size distributions (right column of figures). Site scale expectations are the means of plot-scale expectations from the best model for all plots. LiDAR-estimated site leaf area profiles (red) are compared with model predictions (black). Observed tree counts in size bins (red circles) are plotted against model expectations (black lines). For comparison, each other site's model expectations are plotted as thin light blue lines in size distribution panels. Expectations significantly captured plot and site level variation in observed leaf area profile and size distributions (see text). Dashed grey lines are ideal Metabolic Scaling Theory predictions.

have lead plastic canopies to reorganise to escape low-light environments and create a distinct canopy layer. The relative openness of the Tapajós suggests that plasticity may not

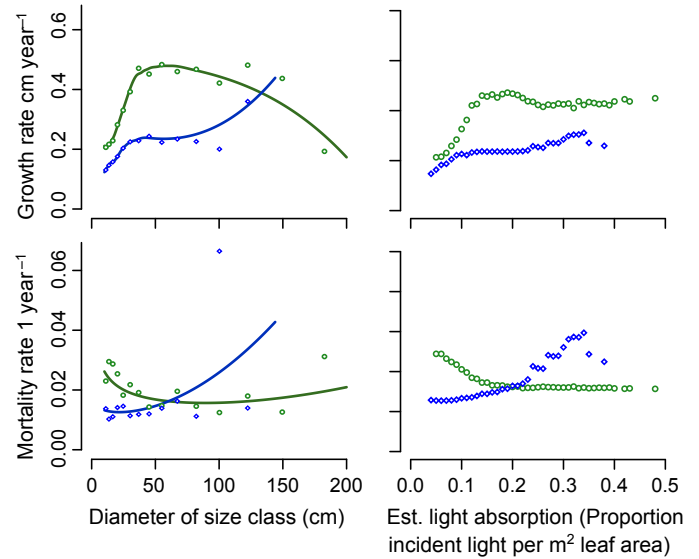


Figure 4 Relationships between growth and mortality rates and stem diameter and mean estimated light environments of size groups. Light absorption was estimated from Model II output for Tapajós (green) and Ducke (blue, diamonds) sites. Left column of panels: solid lines are curves that were fit to individual tree data while open circles are empirical mean values calculated for data visualisation using logarithmically scaled size bins, which were chosen to reduce the number of bins containing < 20 trees. Right column of panels: open circles correspond with light absorption class means (absorption bins 0.01 units wide) over size groups vs. growth (top) and mortality (bottom).

always create continuous canopy layers as is sometimes assumed by perfect plasticity models (Purves *et al.* 2007; Strigul *et al.* 2008). A disturbance prior to 1999 in the Tapajós could have significantly opened the canopy (see Saleska *et al.* 2003; Vieira *et al.* 2004; Pyle *et al.* 2008). Alternatively, higher long-term average mortality rates may prevent the formation of a canopy layer by promoting gap formation or by reducing the number of trees that reach large sizes. In this latter case,

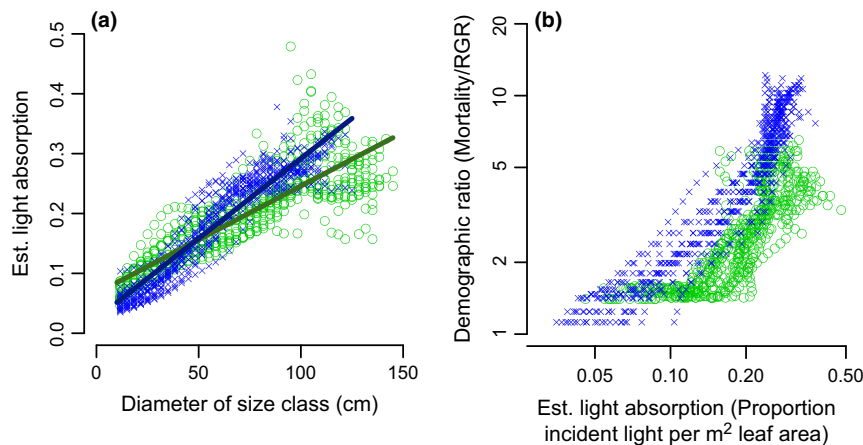


Figure 5 Size group light environments estimated from Model II output vs. diameter classes (panel a) and vs. demographic ratios (panel b) for Tapajós (green) and Ducke (blue) sites. Demographic ratios were calculated from fit growth and mortality curves presented in Fig. 4. In panel (b) axes have been log transformed such that parallel relationships would indicate proportionality. Lower average demographic ratio values in the Tapajós result from relatively higher RGR values. Linear models have been added for each site to panel (a).

reduced competition among larger individuals could play a role promoting the large maximum tree size of the Tapajós, though other explanations for this pattern cannot be ruled out.

We found evidence that demographic rates were related to light environments by linking tree survey data with model output – our best forest structure model provided a hypothesis for how light absorption and leaf area profiles were partitioned over tree size classes. This light estimation approach improves on past work (e.g. Stark *et al.* 2012) by accounting for a complex vertically overlapping pattern of canopy vegetation association with size classes. While patterns of growth were consistent with light limitation (H2) over ranges of low light availability, there was a more general pattern of the demographic ratio increasing over light environment estimates, indicating an increase in the importance of mortality relative to growth in higher light environments. MST, in contrast, incorrectly predicted that the demographic ratio would remain constant over light environments (see Muller-Landau *et al.* 2006b). A potential role of space competition (H1) cannot, however, be ruled out without taking into account canopy plasticity.

We found evidence, though limited, for a light-mediated feedback between forest structure and demography. After fitting the forest demographic model that included an effect of light to site size distributions, we found qualitative consistency between predicted and empirically estimated patterns of light absorption over diameter. Thus, theory suggested that the more gradual increase in light absorption with diameter in the Tapajós was linked through a demographic effect with the more log–log linear size distribution, and similarly for Ducke that the more rapid increase in light absorption was linked with the higher log-log curvature of the size distribution – though this is a weak test of the hypothesis. This approach did not address the ultimate causes of site differences, such as potential impacts of soil or climate on growth and mortality.

Our approach assumed that a single-date LiDAR measurement can capture demographic processes over decade-scale forest dynamics (see also Stark *et al.* 2012). Forest survey data suggest that size structure has remained consistent through time within and between sites (Rice *et al.* 2004; Castilho *et al.* 2006; Pyle *et al.* 2008; Stark *et al.* 2012). Future time-series of LiDAR (e.g. Kellner & Asner 2014; Srinivasan *et al.* 2014) that coincide with tree survey intervals, will allow for the direct comparison of canopy structure change and demographic dynamics, including at smaller tree-plot scales. We also assumed that light was randomly distributed across leaf area at a given height; however, size classes may be associated non-randomly with light, for example, if higher survival or growth leads to the build up of individuals in higher light understory environments (Nicotra *et al.* 1999). Our approach, however, offers explicit transmission estimates for focal size classes that can be derived from LiDAR data, complementing current forest survey approaches that rely on canopy indices (see Clark & Clark 1992; Grote *et al.* 2013). Light estimation and the association of light with size groups can be improved with 3D radiative transfer modelling and through field validation against within-canopy measurements. Future approaches

should improve stem frequency and vital rate predictions for low probability large size classes.

Coordination between growth and mortality processes could explain the increase in demographic ratio over light environments. In this case, a physiologically based trade-off in growth and survival, previously observed in juvenile trees (e.g. Wright *et al.* 2010), may influence growth and mortality across classes. Higher light size classes may also comprise more mature trees and experience higher age-related mortality rates. Alternatively, higher leaf area allocation in higher light environments, supported by our model comparison analysis, may intensify competition for space and increase mortality relative to growth. Consistent with this, and providing some support for space competition, the highest mortality at each site was associated with dense leaf area environments, which fell at contrasting extremes of leaf area profiles (compare mortality in Fig. 4 with leaf area profiles in Fig. 3). Few direct measurements of leaf allocation over light environment and diameter are available to test this hypothesis, highlighting a critical knowledge gap (Valladares & Niinemets 2008) (SI 2.0).

This study improves investigation into feedbacks between forest canopies and demographic processes. While forest demographic theory connects tree demography with size structure (Kohyama 1993; Muller-Landau *et al.* 2006b), the quantitative connection of these factors with canopy structure has remained underdeveloped, probably due to a lack of canopy data acquisition technologies like LiDAR. Prior approaches have forgone explicit consideration of canopy structure for simpler approaches based on height and the basal area of neighbors (Kohyama 1993; Muller-Landau *et al.*, 2006a, b). The explicit consideration of structure, however, has significant advantages: the first is that it enables small footprint LiDAR to infer size distributions and to study demographic dynamics, as this study demonstrates, because LiDAR provides direct data on three-dimensional forest structure (Lefsky *et al.* 2002). This offers a foundation for rapid and large scale prediction of forest size structure and demographic dynamics – a high throughput approach for forest ecology that complements the development of LiDAR for monitoring of biomass dynamics (e.g. Asner *et al.* 2010). The second major advantage is that canopy structure is directly related to canopy function, surface energy balance dynamics, and forest-atmosphere feedbacks (Parker *et al.* 2004; Medvigy *et al.* 2009). Increasingly, dynamic vegetation models include forest structure and demography to better predict future climates and vegetation climate responses. The Ecosystem Demography model, for example, explicitly connects size distributions with canopy structure but under the unrealistic assumption that a tree size class occupies a single narrow canopy strata (Moorcroft *et al.* 2001; Medvigy *et al.* 2009), which disagrees with the complex vertically overlapping pattern of vegetation supported by our best model. This may lead to the improper characterisation of light vs. carboxylation limitation over leaf area, biasing ED production estimates.

LiDAR has been employed to estimate tropical forest structural parameters such as total leaf area, basal area, biomass and biomass change (Harding *et al.* 2001; Parker, *et al.*, 2001, 2004; Drake *et al.* 2002; Kellner & Asner 2009, 2014; Stark

et al. 2012; Tang *et al.* 2012) and to improve the application of vegetation models (Antonarakis *et al.* 2011). This study builds on this past work while uniquely focusing on the size distribution of trees (but see also Antonarakis *et al.* 2014; Srinivasan *et al.* 2014). Past LiDAR approaches have often focused on canopy-top gap dynamics or canopy height distributions (see Antonarakis *et al.* 2011; Kellner & Asner 2014) while our approach, in contrast, focuses on the demographic dynamics of groups that occupy both canopy and sub canopy positions and relies on LiDAR pulse penetration over the full canopy profile.

This study showed that the rapid remote detection of canopy structure can be used to predict size distributions and forest dynamics, suggesting the possibility of future investigations of these factors on unprecedented scales. Applied with multi-temporal LiDAR, this approach would offer a new avenue to investigate climate change consequences in climatically critical forests such as the Amazon. Furthermore, this study and approach improves understanding of the light-mediated feedback between forest structure and tree demography, a critical component of theory of the biosphere and vegetation–atmosphere interactions.

AUTHORSHIP

SCS designed the research, collected data, conducted analysis, and developed the manuscript. BJE contributed to research design, to data analysis, and to manuscript development. SRS contributed to overall research design, manuscript development, and to airborne LiDAR data acquisition. VL, JS, ML, LFA, PBC and RCO collected data, contributed to pre-analysis processing and investigation implementation and commented on the manuscript during development.

ACKNOWLEDGEMENTS

This work was supported by National Science Foundation awards (DDIG 0807221, DEB 0721140, OISE-PIRE 0730305, DEB-MSB 1340604) and the National Air and Space Administration (contract NNX09AI33G) while Stark was also supported by NSF GRFP and NSF PIRE fellowships. Extensive scientific field and logistical support were provided by administrators and technicians associated with the Brazilian institutions INPA-LBA, Embrapa Amazônia Oriental, INPA-Biodiversity, and PPBio/CENBAM, as well as local communities, in Santarém and Manaus. We acknowledge anonymous reviewers and members of the Saleska lab (U of A) and Kobe lab (MSU) for their excellent feedback that improved this manuscript.

REFERENCES

Antonarakis, A., Saatchi, S., Chazdon, R. & Moorcroft, P. (2011). Using lidar and radar measurements to constrain predictions of forest ecosystem structure and function. *Ecol. Appl.*, 21, 1120–1137.

Antonarakis, A., Munger, J. & Moorcroft, P. (2014). Imaging spectroscopy and lidar-derived estimates of canopy composition and structure to improve predictions of forest carbon fluxes and ecosystem dynamics. *Geophys. Res. Lett.*, 41, 2535–2542.

Asner, G., Powell, G., Mascaro, J., Knapp, D., Clark, J., Jacobson, J. *et al.* (2010). High-resolution forest carbon stocks and emissions in the Amazon. *Proc. Natl. Acad. Sci. USA*, 107, 16738.

Brokaw, N. (1985). Gap-phase regeneration in a tropical forest. *Ecology*, 66, 682–687.

Castilho, C., Magnusson, W., Araújo, R., Luizão, R., Luizão, F., Lima, A. *et al.* (2006). Variation in aboveground tree live biomass in a central Amazonian forest: effects of soil and topography. *Forest Ecol. Manag.*, 234, 85–96.

Chambers, J., Higuchi, N., Teixeira, L., dos Santos, J., Laurance, S. & Trumbore, S. (2004). Response of tree biomass and wood litter to disturbance in a central amazon forest. *Oecologia*, 141, 596–611.

Clark, D. & Clark, D. (1992). Life history diversity of canopy and emergent trees in a neotropical rain forest. *Ecol. Monogr.*, 62, 315–344.

Coomes, D., Lines, E. & Allen, R. (2011). Moving on from metabolic scaling theory: hierarchical models of tree growth and asymmetric competition for light. *J. Ecol.*, 99, 748–756.

Coomes, D., Holdaway, R., Kobe, R., Lines, E. & Allen, R. (2012). A general integrative framework for modelling woody biomass production and carbon sequestration rates in forests. *J. Ecol.*, 100, 42–64.

Drake, J., Dubayah, R., Knox, R., Clark, D. & Blair, J. (2002). Sensitivity of large-footprint lidar to canopy structure and biomass in a neotropical rainforest. *Remote Sens. Environ.*, 81, 378–392.

Enquist, B. & Niklas, K. (2002). Global allocation rules for patterns of biomass partitioning in seed plants. *Science*, 295, 1517–1520.

Enquist, B.J., West, G.B., Charnov, E.L. & Brown, J.H. (1999). Allometric scaling of production and life-history variation in vascular plants. *Nature*, 401, 907–911.

Enquist, B., West, G. & Brown, J. (2009). Extensions and evaluations of a general quantitative theory of forest structure and dynamics. *Proc. Natl. Acad. Sci. USA*, 106, 7046.

Feldpausch, T., Banin, L., Phillips, O., Baker, T., Lewis, S., Quesada, C. *et al.* (2010). Height-diameter allometry of tropical forest trees. *Biogeosciences*, 7, 7727–7793.

Grote, S., Condit, R., Hubbell, S., Wirth, C. & Rüger, N. (2013). Response of demographic rates of tropical trees to light availability: can position-based competition indices replace information from canopy census data? *PloS One*, 8, e81787.

Harding, D., Lefsky, M., Parker, G. & Blair, J. (2001). Laser altimeter canopy height profiles: methods and validation for closed-canopy, broadleaf forests. *Remote Sens. Environ.*, 76, 283–297.

Horn, H. (1971). *Adaptive Geometry of Trees. Monographs in Population Biology 3*. Princeton University Press, Princeton, NJ.

Kellner, J. & Asner, G. (2009). Convergent structural responses of tropical forests to diverse disturbance regimes. *Ecol. Lett.*, 12, 887–897.

Kellner, J.R. & Asner, G.P. (2014). Winners and losers in the competition for space in tropical forest canopies. *Ecol. Lett.*, 17, 556–562.

Kohyama, T. (1993). Size-structured tree populations in gap-dynamic forest—the forest architecture hypothesis for the stable coexistence of species. *J. Ecol.*, 81, 131–143.

Lefsky, M., Cohen, W., Parker, G. & Harding, D. (2002). Lidar remote sensing for ecosystem studies. *Bioscience*, 52, 19–30.

MacArthur, R. & Horn, H. (1969). Foliage profile by vertical measurements. *Ecology*, 50, 802–804.

Magnusson, W., Lima, A., Luizão, R., Luizão, F., Costa, F., Castilho, C. *et al.* (2005). RAPELD: a modification of the Gentry method for biodiversity surveys in long-term ecological research sites. *Biota Neotropica*, 5, 19–24.

Medvigy, D., Wofsy, S., Munger, J., Hollinger, D. & Moorcroft, P. (2009). Mechanistic scaling of ecosystem function and dynamics in space and time: Ecosystem Demography model version 2. *J. Geophys. Res.*, 114, G01002.

Monteith, J. (1965). Light distribution and photosynthesis in field crops. *Ann. Bot-London*, 29, 17–37.

Moorcroft, P. (2006). How close are we to a predictive science of the biosphere? *Trends. Ecol. Evol.*, 21, 400–407.

- Moorcroft, P., Hurtt, G. & Pacala, S. (2001). A method for scaling vegetation dynamics: the ecosystem demography model (ED). *Ecol. Monogr.*, 71, 557–586.
- Muller-Landau, H., Condit, R., Chave, J., Thomas, S., Bohlman, S., Bunyavejchewin, S. *et al.* (2006a). Testing metabolic ecology theory for allometric scaling of tree size, growth and mortality in tropical forests. *Ecol. Lett.*, 9, 575–588.
- Muller-Landau, H., Condit, R., Harms, K., Marks, C., Thomas, S., Bunyavejchewin, S. *et al.* (2006b). Comparing tropical forest tree size distributions with the predictions of metabolic ecology and equilibrium models. *Ecol. Lett.*, 9, 589–602.
- Nicotra, A., Chazdon, R. & Iriarte, S. (1999). Spatial heterogeneity of light and woody seedling regeneration in tropical wet forests. *Ecology*, 80, 1908–1926.
- Parker, G., Lefsky, M. & Harding, D. (2001). Light transmittance in forest canopies determined using airborne laser altimetry and in-canopy quantum measurements. *Remote Sens. Environ.*, 76, 298–309.
- Parker, G., Harmon, M., Lefsky, M., Chen, J., Pelt, R., Weiss, S. *et al.* (2004). Three-dimensional structure of an old-growth Pseudotsuga-Tsuga canopy and its implications for radiation balance, microclimate, and gas exchange. *Ecosystems*, 7, 440–453.
- Phillips, O., Aragão, L., Lewis, S., Fisher, J., Lloyd, J., López-González, G. *et al.* (2009). Drought sensitivity of the Amazon rainforest. *Science*, 323, 1344.
- Poorter, L., Bongers, F., Sterck, F. & Wöll, H. (2003). Architecture of 53 rain forest tree species differing in adult stature and shade tolerance. *Ecology*, 84, 602–608.
- Purves, D.W., Lichstein, J.W. & Pacala, S.W. (2007). Crown plasticity and competition for canopy space: a new spatially implicit model parameterized for 250 north american tree species. *PLoS One*, 2, e870.
- Pyle, E., Santoni, G., Nascimento, H., Hutryra, L., Vieira, S., Curran, D. *et al.* (2008). Dynamics of carbon, biomass, and structure in two Amazonian forests. *J. Geophys. Res.*, 113, no. G1.
- Rice, A., Pyle, E., Saleska, S., Hutryra, L., Palace, M., Keller, M. *et al.* (2004). Carbon balance and vegetation dynamics in an old-growth Amazonian forest. *Ecol. Appl.*, 14, 55–71.
- Saleska, S., Miller, S., Matross, D., Goulden, M., Wofsy, S., da Rocha, H. *et al.* (2003). Carbon in Amazon forests: unexpected seasonal fluxes and disturbance-induced losses. *Science*, 302, 1554.
- Shinozaki, K., Yoda, K., Hozumi, K. & Kira, T. (1964). A quantitative analysis of plant form—the pipe model theory i. basic analyses. *JPN J. Ecol.*, 14, 97–105.
- Sitch, S., Huntingford, C., Gedney, N., Levy, P., Lomas, M., Piao, S. *et al.* (2008). Evaluation of the terrestrial carbon cycle, future plant geography and climate-carbon cycle feedbacks using five Dynamic Global Vegetation Models (DGVMs). *Global Change Biol.*, 14, 2015–2039.
- Srinivasan, S., Popescu, S.C., Eriksson, M., Sheridan, R.D. & Ku, N.W. (2014). Multi-temporal terrestrial laser scanning for modeling tree biomass change. *Forest Ecol. Manag.*, 318, 304–317.
- Stark, S., Leitold, V., Wu, J., Hunter, M., de Castilho, C., Costa, F. *et al.* (2012). Amazon forest carbon dynamics predicted by profiles of canopy leaf area and light environment. *Ecol. Lett.*, 15, 1406–1414.
- Sterck, F. & Bongers, F. (2001). Crown development in tropical rain forest trees: patterns with tree height and light availability. *J. Ecol.*, 89, 1–13.
- Strigul, N., Pristinski, D., Purves, D., Dushoff, J. & Pacala, S. (2008). Scaling from trees to forests: tractable macroscopic equations for forest dynamics. *Ecol. Monogr.*, 78, 523–545.
- Tang, H., Dubayah, R., Swatantran, A., Hofton, M., Sheldon, S., Clark, D. & Blair, B. (2012). Retrieval of vertical LAI profiles over tropical rain forests using waveform lidar at la selva, costa rica. *Remote Sens. Environ.*, 124, 242–250.
- Valladares, F. & Niinemets, Ü. (2008). Shade tolerance, a key plant feature of complex nature and consequences. *Annu. Rev. Ecol. Evol. Syst.*, 39, 237.
- Vieira, S., De Camargo, P., Selhorst, D., Da Silva, R., Hutryra, L., Chambers, J. *et al.* (2004). Forest structure and carbon dynamics in Amazonian tropical rain forests. *Oecologia*, 140, 468–479.
- West, G., Enquist, B. & Brown, J. (2009). A general quantitative theory of forest structure and dynamics. *Proc. Natl. Acad. Sci. USA*, 106, 7040.
- Wright, S., Kitajima, K., Kraft, N., Reich, P., Wright, I., Bunker, D. *et al.* (2010). Functional traits and the growth-mortality trade-off in tropical trees. *Ecology*, 91, 3664–3674.
- Young, T. & Hubbell, S. (1991). Crown asymmetry, treefalls, and repeat disturbance of broad-leaved forest gaps. *Ecology*, 72, 1464–1471.

SUPPORTING INFORMATION

Additional Supporting Information may be downloaded via the online version of this article at Wiley Online Library (www.ecologyletters.com).

Editor, Maria Uriarte

Manuscript received 25 September 2014

First decision made 7 November 2014

Second decision made 21 February 2014

Manuscript accepted 23 March 2015